J. Membrane Biol. 206, 227–238 (2005)
DOI: 10.1007/s00232-005-0796-x

The Journal of
Membrane
Biology

Functionally Important Residues in the Predicted 3rd Transmembrane Domain of the Type IIa Sodium-phosphate Cotransporter (NaPi-IIa)

L.V. Virkki, I.C. Forster, A. Bacconi, J. Biber, H. Murer
Institute of Physiology and Center for Integrative Human Physiology, University of Zürich, Winterthurerstrasse 190, CH-8057, Zürich, Switzerland

Received: 22 July 2005/Accepted: 22 September 2005

Abstract. The type IIa Na^+/P_i, cotransporter (NaPi-IIa) mediates electrogenic transport of three Na^+ and one divalent P_i ion (and one net positive charge) across the cell membrane. Sequence comparison of electrogenic NaPi-IIa and IIb isoforms with the electroneutral NaPi-IIc isoform pointed to the third transmembrane domain (TMD-3) as a possibly significant determinant of substrate binding. To elucidate the role of TMD-3 in the topology and mechanism underlying NaPi-IIa function we subjected it to cysteine scanning mutagenesis. The constructs were expressed in *Xenopus* oocytes and P_i transport kinetics were assayed by electrophysiology and radiotracer uptake. Cys substitution resulted in only marginally altered kinetics of P_i transport in those mutants providing sufficient current for analysis. Only one site, at the extracellular end of TMD-3, appeared to be accessible to methanethiosulfonate reagents. However, additional mutations carried out at D224 (replaced by E, G or N) and N227 (replaced by D or Q) resulted in markedly altered voltage and substrate dependencies of the P_i-dependent currents. Replacing Asp-224 (highly conserved in electrogenic a and b isoforms) with Gly (the residue found in the electroneutral c isoform) resulted in a mutant that mediated electroneutral Na^+-dependent P_i transport. Since electrogenic NaPi-II transports 3 Na^+/transport cycle, whereas electroneutral NaPi-IIc only transports 2, we speculate that this loss of electrogenicity might result from the loss of one of the three Na^+ binding sites in NaPi-IIa.

Key words: Structure-function — Cysteine scanning — Stoichiometry — Electrophysiology — Voltage clamp

Correspondence to: L.V. Virkki; email: leilav@physiol.unizh.ch

Introduction

The physiological role of type II sodium-phosphate cotransporters is to facilitate cellular uptake of inorganic phosphate (P_i) by coupling it to the transmembrane Na^+ gradient. Three different Na/P_i cotransporter isoforms are known to date. The type IIa cotransporter (NaPi-IIa) is predominantly expressed in brush border membranes of the kidney proximal tubule and is a major contributor to regulated P_i reabsorption [17, 18, 23]. The type IIb cotransporter is expressed in (among other tissues) the intestine, where it mediates P_i absorption from the gut lumen [4, 9]. Similar to the IIa isoform, the recently cloned type IIc cotransporter is expressed in the kidney proximal tubule and is strongly upregulated in response to a low-P_i diet [21, 22]. The main functional difference between the isoforms is that, whereas type IIa and IIb cotransporters are electrogenic, type IIc is electroneutral.

Topology analyses based on hydropathy plots and hidden-Markov modeling predict at least eight transmembrane domains (TMDs) for type II Na/P_i, cotransporters (*see* Fig. 1). Intracellular orientation of the N and C termini have been verified using epitope tagging, as has the extracellular location of a large glycosylated loop between TMDs 3 and 4 [8, 16]. Substituted cysteine accessiblity mutagenesis (SCAM) studies suggested that the long linking regions between TMDs 2–3 and 5-6 enter the membrane to form part of the transport corridor [6, 10, 11, 15]. Also the short external loops connecting TMDs 2-3 and 7-8 contain functionally sensitive sites important with respect to defining the voltage sensitivity of NaPi-IIa [2, 3].

Sequence comparison between the different isoforms shows that amino acids in the putative TMDs and in the two re-entrant loops are highly conserved. Moreover, a comparison of all currently available

sequence data reveals that there are very few non-conservative substitutions between the electrogenic and electroneutral isoforms [1]. One prominent substitution appears in TMD-3, where Asp-224 (numbering based on human NaPi-IIa) in the electrogenic IIa and IIb isoforms is substituted with a glycine in the electroneutral IIc. Since TMD-3 is also amphipathic and could therefore form part of an aqueous transport pathway, we hypothesized that this TMD might be important in substrate recognition and transport function in Na/P_i cotransporters. In this study we therefore focussed on TMD-3 by first performing cysteine scanning mutagenesis of 19 consecutive amino acids predicted to constitute TMD-3 and second, investigating the effects of mutagenesis at sites highlighted from bioinformatic considerations.

Materials and Methods

Molecular Biology and Oocyte Expression

The cDNA encoding human NaPi-IIa (*NPT2a*, SLC34A1) was previously subcloned into a KSM expression vector to improve its expression in *Xenopus laevis* oocytes [26]. Mutant transporters were generated using the Quickchange Site-directed Mutagenesis kit (Stratagene) according to manufacturer's directions. Mutants were verified by sequencing (Microsynth). Before introducing novel Cys residues in TMD-3, we first replaced the native Cys-225 with Ser (C225S). All mutants in which we introduced a novel Cys were constructed on this C225S backbone, all other mutants were constructed on the wild-type (WT) backbone. The plasmids were linearized using Xba1 (Promega) and used as a template for the synthesis of capped cRNA using the Message Machine T3 kit (Ambion).

Stage V-VI defolliculated oocytes from *Xenopus laevis* were isolated and maintained as described previously [27]. Oocytes were injected with 50 nl of cRNA (0.2 μg/μl) encoding WT or mutant NaPi-IIa. Control oocytes were injected with 50 nl of water. Oocytes were incubated at +18°C in modified Barth's solution, containing (in mM) 88 NaCl, 1 KC1, 0.41 $CaCl_2$, 0.82 $MgSO_4$, 2.5 $NaHCO_3$, 2 $Ca(NO_3)_2$, 7.5 HEPES, pH 7.5 adjusted with TRIS. The solution was supplemented with 5 mg/l doxycyclin. Electrophysiology and radiotracer flux experiments were performed 2–5 days after injection. Each data set is obtained from at least two batches of oocytes from two different donor frogs.

Two-Electrode Voltage Clamp

We used a custom-built voltage clamp optimized for fast clamping speed [5] to make recordings from control oocytes and oocytes expressing WT NaPi-IIa or mutants. The voltage clamp was controlled and data aquired using a computer running pClamp 8 software (Axon Instruments), which also controlled valves for solution switching. Solutions were cooled to 20–22°C before introduction to the oocyte recording chamber at a rate of 5 ml min^{-1}. The oocyte was initially superfused with ND100 solution, containing (in mM) 100 NaCl, 2 KCl, 1.8 $CaCl_2$, 1 $MgCl_2$, 10 HEPES, titrated to pH 7.4 using TRIS. We obtained different concentrations of P_i by adding K_2HPO_4/KH_2PO_4 in proportions giving the desired pH. In some experiments it was necessary to substitute $CaCl_2$ with $BaCl_2$ to suppress the activation of endogenous Cl^- channels at hyperpolarizing voltages. In solutions where the Na^+ concentration was varied (ND0-ND100), NaCl was substitued equimolarly with choline Cl. In some experiments, we replaced NaCl with Na glucuronate to reduce the external Cl^- concentration.

Measurement of Apparent P_i and Na^+ Affinities

The oocyte was clamped to a membrane potential of −50 mV and the holding current was continuously recorded. To measure P_i-induced currents (I_{Pi}), the superfusate was switched to one containing P_i and deflection in the holding current was monitored. When the current had reached its maximum, the perfusate was switched back and washout of P_i was monitored by observing the return of holding current to baseline. When I_{Pi} were to be recorded for another Na^+ concentration or pH, the holding current was first allowed to stabilize in the new baseline solution before switching to one including P_i. For determining the apparent K_m for P_i, P_i-induced current deflections were measured using different P_i concentrations while keeping the Na^+ concentration constant. For determining the apparent K_m for Na^+, the oocyte was first perfused with a specific concentration of Na^+ before switching to a solution containing P_i in the same solution (the P_i concentration was kept constant throughout the experiment)

The apparent K_m for P_i and Na^+ was determined by fitting data with the modified Hill equation:

$$I_{Pi} = I_{Pi,\,max}\,[S]^H/([S]^H + (K_m)^H) \quad (1)$$

where I_{Pi} is the P_i-induced current, $I_{Pi,max}$ is the extrapolated maximal P_i-induced current, $[S]$ is the concentration of substrate (Na^+ or P_i), K_m is the concentration of substrate that gives half-maximum response, and H is the Hill coefficient. For determining K_mP_i, H was constrained to 1.

Incubation with Methanethiosulfonate (MTS) Reagents

Sodium (2-sulfonatoethyl)methane thiosulfonate (MTSEA), [2-(trimethylammonium) ethyl]methanethiosulfonate bromide (MTSET) and sodium (2-sulfonatoethyl)methane thiosulfonate (MTSES) were dissolved in DMSO at a concentration of 1 M and stored at −20°C. Immediately before use, the MTS reagents were diluted to a final concentration of 1 mM in ice-cold ND100 solution and applied using gravity feed through a stainless-steel cannula placed close to the oocyte. During application, the oocyte was held at −50 mV and the current tracing monitored continuously. Before MTS application, I_{Pi} was measured using 1 mM P_i in ND100 solution.

Measuring the Voltage-dependency of P_i-induced Currents

The voltage-dependency of P_i- induced currents was measured by applying holding potentials from −160 or −140 mV to +40 mV and recording currents in the presence and absence of P_i, as described previously [5]. For determining the P_i -dependency of the current, we varied the P_i concentration while keeping the Na^+ concentration constant. For determining the Na^+-dependency of the current, the oocyte was first perfused with a specific concentration of Na^+ and subsequent recordings were obtained in the presence and absence of P_i. In both cases, current records obtained in the absence of P_i were subtracted from those recorded in the presence of P_i to obtain the P_i-dependent current. To compensate for the differences in expression levels between individual oocytes,

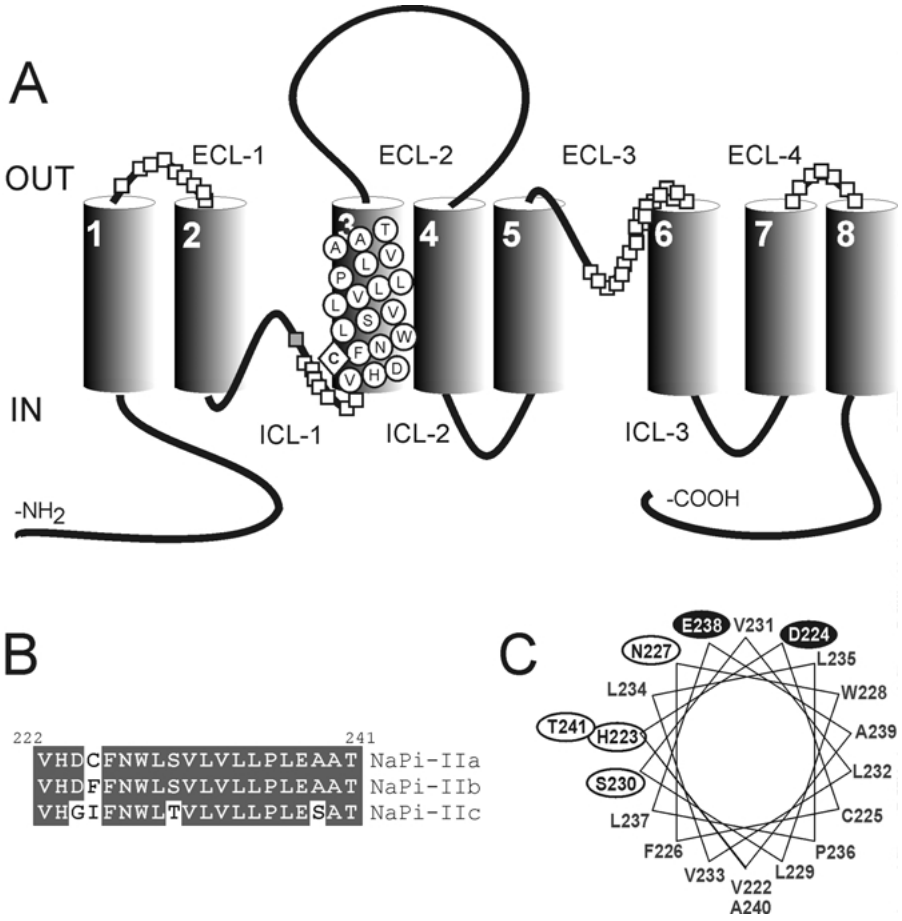

Fig. 1. Topology and sequence alignment. (*A*) Topology model of human NaPi-IIa contains eight putative transmembrane segments and intracellular N and C termini. Open squares indicate residues in the extracellular and intracellular linker regions (ECL and ICL, respectively) that were mutated in previous cysteine scanning accessibility studies [2, 3, 10, 15]. Of these, Asn-199, which is postulated to interact with sites in TMD-3, is indicated with a grey sqare. Residues mutated to cysteines in TMD-3 (this study) are indicated by a letter corresponding to the amino acid in a white circle. The native Cys-225 (denoted by a diamond) was changed to Ser. (*B*) Alignment of the amino acid sequence in TMD-3 of human NaPi-IIa, IIb and IIc. Non-conserved residues are indicated by black lettering on white background. (*C*) Helical wheel analysis of TMD-3 in NaPi-IIa. Charged residues are indicated by white lettering in a black oval and polar residues by black lettering inside a white oval.

the data obtained from each oocyte were normalized to the Pi-dependent current recorded at −100 mV with 100 mM Na^+ and 1 mM P_i in the bath at pH 7.4 before fitting the data with Eq. 1 plus a variable offset. The offset is included to account for the leak current, which is present in NaPi-IIa-expressing oocytes in the absence of P_i, but blocked by P_i with an unknown affinity [2, 25].

Radiotracer uptake

A group of oocytes (5–9 oocytes/group) was first allowed to equilibrate in uptake solution without tracer. After aspiration of as much of this solution as possible, we added 100 μl uptake solution containing radiotracer ($^{32}P_i$, ^{22}Na or both). The uptake was allowed to proceed for 15–30 min before it was stopped by washing the oocytes three times with 4 ml ice-cold ND0 solution containing 2 mM cold P_i. If no P_i was present in the uptake solution, washing was performed with ice-cold ND0 solution.

Uptake of $^{32}P_i$ alone was carried out using ND100 solution and 1 mM cold P_i, to which $^{32}P_i$ (^{32}P-orthophosphate, specific activity 10 mCi/mmol P_i) was added. For dual uptake of both $^{32}P_i$ and ^{22}Na, it was necessary to lower the Na^+ concentration to achieve a high enough specific activity for Na^+. Therefore these experiments were carried out using ND40 solution with 2–3 mM cold P_i, and containing the isotopes ^{32}P-orthophosphate (specific activity 3 mCi/mmol P_i) and ^{22}Na (specific activity 350 μCi/mmol Na; Amersham).

After washing, oocytes were placed individually in a scintillation vial and lysed in 250 μl 10% SDS. ^{32}P and ^{22}Na activities of individual oocytes were counted using a Packard Tri-Carb 2900TR scintillation counter. For the dual uptake experiments the counts of the two isotopes were separated using a Dual DPM assay with quench curves.

Western Blotting

Pools of three oocytes were lysed in 60 μl homogenization buffer (100 mM NaCl, 200 mM Tris-HCl, 3% pentaethyleneglycol mono-*n*-dodecyl ether (Calbiochem), pH 7.6). Yolk proteins were removed by centrifugation (3 min 16,000 × *g*). 10 μl supernatant was mixed with 10 μl loading buffer (380 mM Tris-HCl, 8% SDS, 4 mM EDTA, 40% glycerol, 4 mg/ml bromophenol blue, pH 6.8) and separated on a 9% SDS-PAGE gel. Separated proteins were

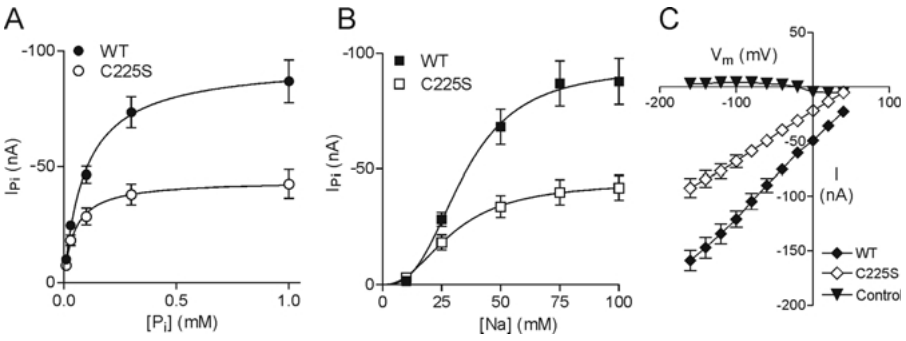

Fig. 2. Characterization of the C225S mutant. (*A*) P_i dose-response. The P_i-induced current was plotted as a function of P_i concentration. *Filled circles*, WT; *empty circles*, C225S. The data were fitted with Eq. 1, yielding the following fit parameters: for WT, K_mP_i = 0.094 ± 0.02 mM, $I_{Pi,\ max}$ = 95 ± 6 nA; for C225S, K_mP_i = 0.047 ± 0.02, $I_{Pi,\ max}$ = 44 ± 4 nA, n = 10. (*B*) Na^+ dose-response. The P_i-induced current was plotted as a function of the Na^+ concentration. *Filled squares*, WT; *empty squares*, C225S. The data was fitted with Eq. 1, yielding for the WT, K_mNa = 34 ± 5 mM, H = 2.8 ± 0.9, $I_{Pi,\ max}$ = 94 ± 11 nA; for C225S, K_mNa = 30 ± 7 mM, H = 2.3 ± 1, $I_{Pi,\ max}$ = 44 ± 7nA, n = 5. (*C*) Current-voltage relationship. Current recordings were acquired in ND100 solution in the presence or absence of 1 mM P_i, and subtracted to obtain the P_i-dependent current, which was plotted as a function of voltage. *Filled diamonds*, WT; *empty diamonds*, C225S; *filled triangles*, control oocytes. n = 5–7.

transferred onto a nitrocellulose membrane (Schleicher & Schuell). The membrane was preincubated in blotting solution (5% nonfat milk in 100 mM NaCl, 50 mM Tris-HCl, pH 7.4) and then probed for NaPi-IIa protein using a rabbit polyclonal antibody raised against a synthetic C-terminal peptide (dilution 1:2000 in blotting solution). Signal was detected by incubating the blot with a horseradish peroxidase-conjugated F(ab')2 fragment (Amersham) and then exposing it to a solution containing 0.0165% H_2O_2, 1.25 mM luminol and 0.2 mM p-coumaric acid in 100 mM Tris-HCl, pH 8.5. Chemiluminescence was detected using autoradiography.

Reagents

All standard chemicals and reagents were obtained from either Sigma or Fluka Chemie AG. ^{32}P-orthophosphate was purchased from New England Nuclear and ^{22}Na was from Amersham. The Cys-reactive reagents MTSEA, MTSET and MTSES were from Toronto Research Chemicals.

Data Presentation and Statistical Analysis

All data is shown as means ± SEM, where n denotes the number of experiments. Error bars are not shown when they are smaller than the symbols. Statistical analysis of the data was carried out using two-tailed t-test or one-tailed ANOVA with Tukey's post-test, with $p < 0.05$ considered significant. Both statistical analysis and curve fitting were done using GraphPad Prism 3.0 software (GraphPad Software).

Results

Cysteine Scanning Mutagenesis in TMD-3

Our first strategy to determine structure-function relationships in TMD-3 was to perform cysteine scanning mutagenesis (SCAM). TMD-3 contains one native Cys (C225), which was removed to avoid possible interaction between this Cys and newly introduced residues, or the possibility that the mutagenesis would change the reactivity of C225S by making it more exposed. To establish the feasibility of using this substitution as a backbone for the subsequent cysteine scanning mutagenesis (SCAM), we first compared the P_i- and Na^+- activation kinetics of WT and C225S-expressing oocytes at a holding potential of −50 mV. The P_i-induced currents (I_{Pi}) at 100 mM Na^+ were obtained by subtracting the steady-state current in 0 mM P_i from that at the given P_i. The data were easily fit with a Michaelis-Menten function (Eq. 1, H = 1) (Fig. 2*A*). The fitting algorithm reported that the apparent affinity constant for P_i (K_mP_i) was significantly reduced for the C225S mutant (47 ± 16 μM), compared to the WT (94 ± 22 μM, n = 10 each). Furthermore, the maximum P_i-dependent current was approximately halved for C225S, compared to WT.

The corresponding Na^+-activation at 1 mM P_i is shown in Fig. 2*B*. As we have previously reported for the human WT NaPi-IIa [25], C225S also displayed a clear sigmoidicity for I_{Pi} with increasing [Na^+]. Fitting these data with Eq. 1 (H unconstrained) indicated a small but statistically significant decrease in K_mNa in the C225S mutant (30 ± 7 mM), compared to the WT (34 ± 5 mM), n = 5. For WT and C225S, H was 2.8 ± 0.9 and 2.2 ± 1, respectively, consistent with cooperative Na^+ interaction with the protein. Moreover, we observed that the maximum P_i-dependent current mediated by the C225S mutant was half that of the WT, consistent with the P_i-activation data.

To determine if the voltage-dependency of P_i transport was affected by the C225S mutation, we measured I_{Pi} at different voltages. Figure 2*C* shows the current-voltage (*I-V*) relationship for oocytes expressing WT or C225S NaPi-IIa. The current at each voltage was reduced for the C225S mutant, as

compared to WT, but the shapes of the *I-V* relationships were similar, which indicated that the voltage-dependency was not affected by the mutation. Taken together, these data indicated that the Cys-Ser substitution at 225 was well tolerated, but with an approximately 50% decrease in maximum transport rate.

Using the C225S background, we next substituted, one by one, 19 residues in TMD-3 with Cys (from Val-222 to Thr-241). To identify which mutants were capable of mediating P_i transport we measured $^{32}P_i$ uptake using 1 mM cold P_i and 100 mM Na^+. Figure 3*A* shows P_i uptake in oocytes expressing the various Cys mutants used in this study. The results show that removing the native Cys in TMD-3 (C225S) resulted in an ~50% decrease in P_i uptake, which was consistent with the ~50% decrease in Pi-induced currents shown in Fig. 2. Of the 19 novel Cys mutants engineered on the C225S background, four mutants (D224C-C225S, N227C-C225S, P236C-C225S and E238C-C225S) did not mediate significant P_i transport.

Only one mutant (F226C-C225S) showed the same level of P_i transport as C225S. Of the remaining mutants, six mediated ~50% of the C225S transport activity with the last eight mutants mediating even less.

Next, we measured P_i-induced currents in the Cys mutants at a membrane voltage of −50 mV, to determine if the basic electrogenicity of P_i transport had been affected by the mutagenesis. All mutants that mediated significant $^{32}P_i$ transport in Fig. 3*A* also showed P_i-induced currents. Moreover, to determine if the voltage dependency of P_i transport was altered in any of the novel Cys mutants, we measured P_i-dependent currents at different voltages in oocytes expressing WT or mutant NaPi-IIa. All the functional mutants tested (residues 226, 228-232, 234, 235, 237 and 239-241) had *I-V* relationships similar to those of C225S shown in Fig. 2*C* (*data not shown*).

To assess if the reduction in P_i transport seen in some mutants was due to reduced protein expression, we performed Western blotting on whole-oocyte lysates. Figure 3*B* shows a Western blot of cell lysates of control oocytes and oocytes expressing WT and mutant NaPi-IIa protein. The low-molecular weight band corresponds to the predicted molecular weight of unglycosylated monomeric NaPi-IIa protein (68.9 kD), whereas the weaker band around 80–100 kD corresponds to the glycosylated form. No signal was detectable in the control lane, indicating that the signal in the other lanes is specific for NaPi-IIa.

A comparison of the $^{32}P_i$ uptake data in Fig. 3*A* with the Western blots shown in Fig. 3*B* indicates that only a few mutants expressed at the same level as the WT. Of these, D224C-C225S did not show significant P_i uptake, indicating that although protein was synthesized, it either did not function correctly or was not targeted to the membrane. The only mutants that showed C225S-like expression and at least 50% of its P_i uptake were F226C-C225S, W228C-C225S, S230C-C225S, A239C-C225S and A240C-C225S.

For mutants that showed sufficient P_i-induced currents, we measured K_mP_i to determine if a change in this kinetic parameter could account for the reduced transport activity (Fig. 3*C*).

Most mutants with large enough Pi-induced currents to yield a reliable measurement over the range of P_i concentrations used (0.01 to 1 mM) had similar K_mP_i, compared to C225S. S230C-C225S was the only mutant with a marked increase in K_mP_i (110 ± 10 μM, compared to 47 ± 16 μM for C225S); however, this value is still well below the concentration of P_i used in the uptake study (1 mM). Since S230C-C225S showed an increase in K_mP_i, we decided to also determine K_mNa for this mutant. Its K_mNa was significantly increased at 55 ± 2 mM, compared to 30 ± 7 mM for C225S. Taken together, these results indicated that the reduced P_i transport activity seen in Fig. 3*A* could not be explained by a reduction in P_i affinity.

To perform a cysteine scanning of the novel TMD-3 mutants, we compared I_{Pi} under voltage-clamp conditions (100 mM Na^+, −50 mV) before and after exposure to the methanethiosulfonate (MTS) MTSEA at a concentration of 1 mM, which we have previously used as a benchmark condition to detect Cys residues at functionally important sites, e.g., [3, 15]. Only one mutant, A240C-C225S, showed a change in I_{Pi} after MTSEA treatment for 5 min. For this mutant, I_{Pi} was reduced by ~50%, and no further change in I_{Pi} was obtained even with increasing the treatment period to 15 min (Fig. 3*D*). Similar results were obtained with MTSET (1 mM), which confirmed that the site was accessed from the extracellular compartment. In contrast, applying MTSES for up to 15 min had no effect on P_i-induced currents. Furthermore, A240C-C225S-expressing oocytes previously exposed to MTSES retained their MTSEA sensitivity, indicating that MTSES was unable to react with this novel Cys under these conditions.

Site-directed Mutagenesis at Three Sites in TMD-3

Our second strategy to determine the structure-function relationships in TMD-3 made use of a sequence comparison of this region between electrogenic and electroneutral type II Na/P_i cotransporters (Fig. 1*B*) and the position of three oxygen-containing polar/charged residues on one face of TMD-3 (Fig. 1*C*), which might be involved in Na^+ ion coordination.

Asp-224

The charged residue Asp-224 is conserved among the electrogenic type IIa and IIb Na/P_i cotransporters,

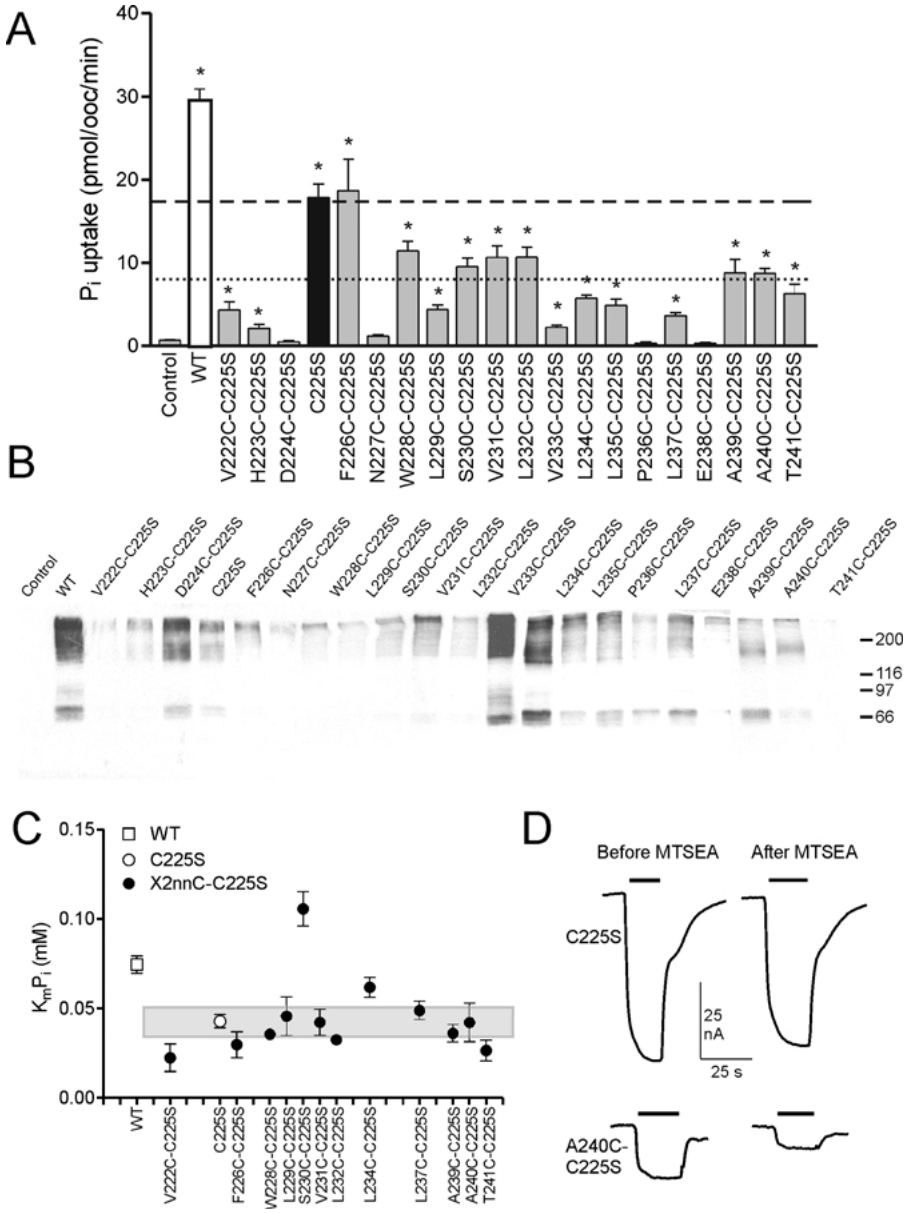

Fig. 3. P_i transport and Western analysis. (*A*) P_i uptake in oocytes expressing WT and mutant NaPi-IIa. P_i uptake was measured using $^{32}P_i$ as a tracer. For clarity, WT is denoted with a white bar, C225S with a black bar, and other mutants with grey bars. The dashed line denotes P_i transport mediated by C225S, and the dotted line, 50% of this. Asterisk * denotes statistically significant difference from control ($P < 0.05$). (*B*) Western blot. Whole-cell lysates from oocytes expressing WT or mutant NaPi-IIa were probed with a NaPi-IIa-specific C-terminal antibody. The sizes of the molecular weight markers are indicated in the figure. The figure is a composition of four separate blots. (*C*) Apparent K_mP_i of WT and mutant NaPi-IIa. WT, *empty square*; C225S, *empty circle*; other mutants, *filled circles*. Grey bar indicates 95% confidence interval for K_mP_i of C225S; $n = 3$–10. (*D*) Effect of MTSEA. Continuous current tracings are shown for oocytes expressing C225S (*top*) or A240C-C225S (*bottom*) before (*left*) or after (*right*) MTSEA treatment (1 mM for 5 min). The recordings were started in ND100 soution, followed by application of 1 mM P_i (indicated by a black line). The P_i-dependent current was determined before and after MTSEA application for each oocyte. MTSEA treatment reduced the Pi-induced current by ~50% in A240C-C225S-expressing oocytes, but not in any other mutants tested.

but is substituted by Gly in the electroneutral NaPi-IIc. To determine if Asp-224 is important for electrogenicity of transport, we made mutations where Asp-224 was substituted with Gly, Glu, or Asn. All mutants mediated P_i transport, as shown by the $^{32}P_i$ uptake assay in Fig. 4*A*, albeit at much reduced rates compared to WT, especially for D224N. Western blotting of total oocyte lysates showed that abundant protein was produced for all mutants (Fig. 4*B*). However, P_i-induced currents were observed for D224E, but not for D224G or D224N (Fig. 4*C*). K_mP_i (measured at −50 mV) for D224E was signifi-

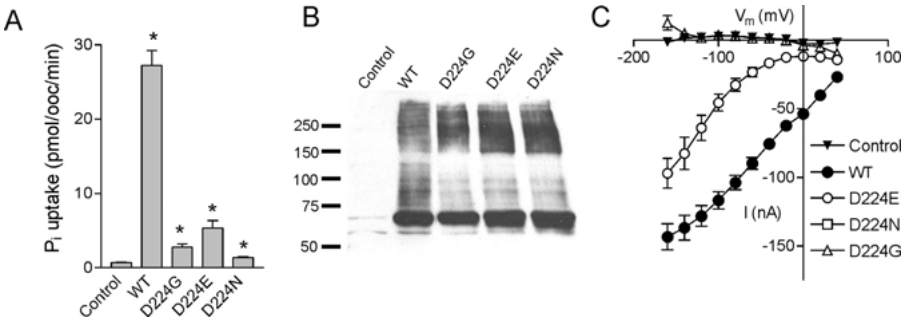

Fig. 4. Mutants at Asp-224. (*A*) P_i uptake. Pi uptake, using $^{32}P_i$ as a tracer, was measured in control oocytes and oocytes expressing mutant engineered at D224 in NaPi-IIa. Asterisk * denotes statistically significant difference from control ($P < 0.05$). (*B*) Western blot. Whole-cell lysates from oocytes expressing WT or mutant NaPi-IIa was probed with a NaPi-IIa-specific antibody. The sizes of the molecular weight markers are indicated in the figure. (*C*) Current-voltage relationships. P_i-induced currents were plotted against membrane potential in control oocytes and oocytes expressing WT or mutant NaPi-IIa. *Filled circles*, WT; *empty circles*, D224E: *empty squares*, D224N, *empty triangles*, D224G, *filled triangles*, control.

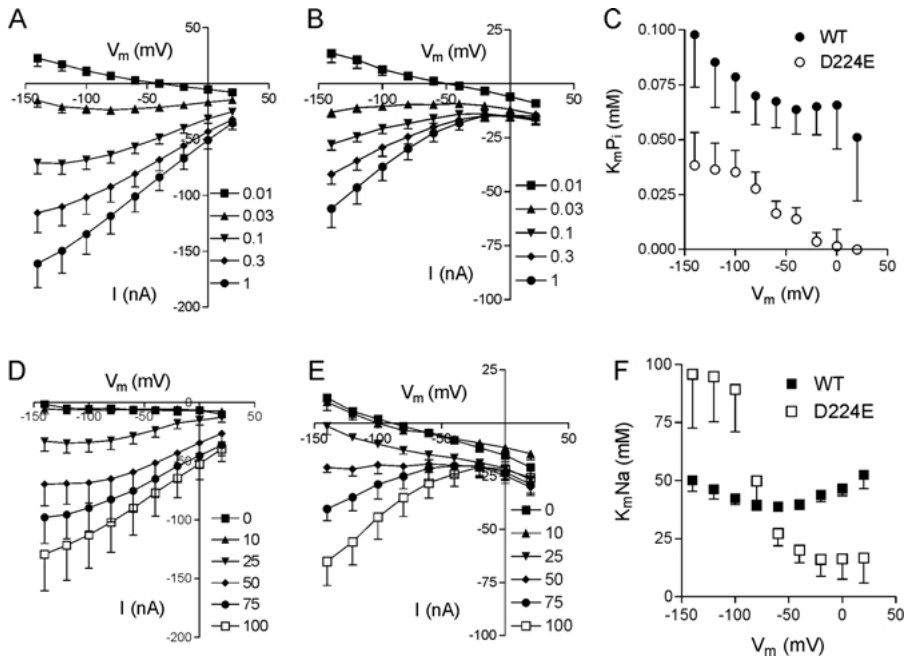

Fig. 5. Voltage-dependency of P_i-induced currents in D224E. (*A*) P_i dose-response in oocytes expressing WT NaPi-IIa. Currents were acquired before and after application of P_i and the P_i-dependent current was plotted as a function of the membrane potential. *Circles*, 1 mM P_i; *diamonds*, 0.3 mM P_i; *inverted triangles*, 0.1 mM P_i; *triangles*, 0.03 mM; *squares*, 0.01 mM P_i. (*B*) P_i dose-response in oocytes expressing D224E. Symbols are as in *A*. (*C*) Voltage-dependency of K_mP_i. Data in panels *A* and *B* were fitted with Eq. 1 and the resulting K_m-values were plotted as a function of voltage. *Filled circles*, WT; *empty circles*, D224E. (*D*) Na^+ dose-response in oocytes expressing WT NaPi-IIa. Currents were acquired before and after application of 1 mM P_i at each Na^+ concentration and the P_i-dependent current was plotted as a function of the membrane potential. *Empty squares*, 100 mM Na^+; *circles*, 75 mM Na^+; *diamonds*, 50 mM Na^+; *inverted triangles*, 25 mM Na^+; *triangles*, 10 mM Na^+; *squares*, 0 mM Na^+. (*E*) Na^+ dose-response in oocytes expressing D224E. Symbols are as in *D*. (*F*) Voltage-dependency of K_mNa. Data in panels *D* and *E* were fitted with Eq. 1 and the resulting K_m-values were plotted as a function of voltage. *Filled squares*, WT; *empty squares*, D224E.

cantly decreased (0.031 ± 0.007 mM, $n = 6$), compared to WT (0.089 ± 0.007 mM). Furthermore, the shape of the *I-V* curve was altered for D224E, so that D224E-mediated P_i-induced currents were clearly voltage dependent only at potentials more negative than −40 mV, whereas currents mediated by WT are voltage-dependent throughout the measurable range (Fig. 4*C*). Removing Cl^- from the bath did not change the shape of the *I-V* curves, which indicates that Cl^- ions did not affect the voltage dependency of P_i transport in this mutant (*not shown*).

We measured P_i-induced currents at different voltages in WT and D224E-expressing oocytes at different concentrations of P_i (at constant 100 mM

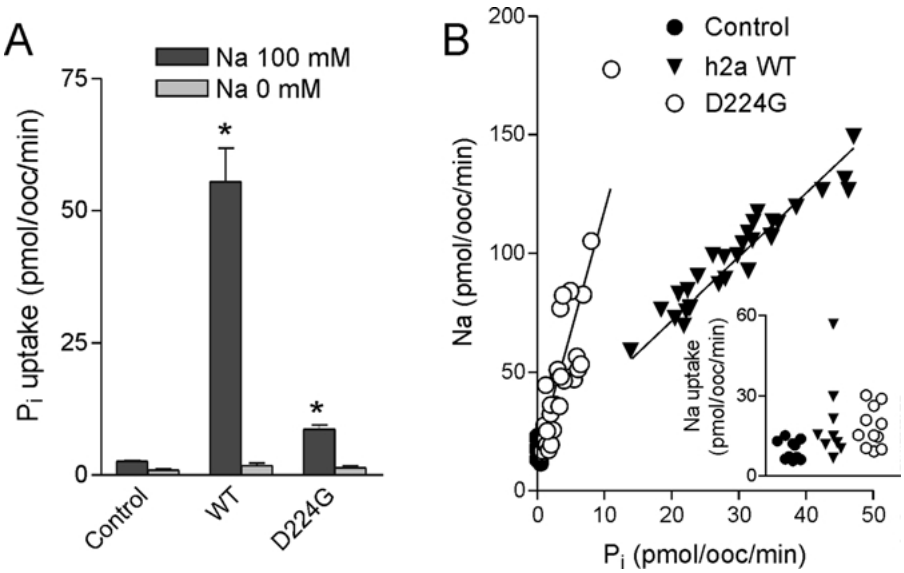

Fig. 6. Transport characteristics by D224G. (*A*) Na^+-dependency of P_i uptake. P_i uptake was measured using $^{32}P_i$ as a tracer, in the presence or absence of Na^+ in control oocytes and oocytes expressing WT or the D224G mutant. Asterisk * denotes statistically significant difference from control ($P < 0.05$). (*B*) Dual uptake of Na^+ and P_i. Simultaneous uptake of Na^+ and P_i (measured using Na^+ and P_i as tracers) in control oocytes (*filled circles*) and in oocytes expressing WT (*filled triangles*) or D224G (*empty circles*) NaPi-IIa. Inset shows Na^+ uptake data for oocytes in the same batch in the absence of P_i. The data were fitted with a regression line (straight lines in graph) with a slope of 2.7 ± 0.04 for WT and 10 ± 0.8 for D224G. The lines were forced to go through the mean values obtained for control oocytes.

Na^+) or Na^+ (at constant 1 mM P_i), and calculated the voltage-dependency of K_mP_i and K_mNa from this data. A comparison of the *I-V* curves in Fig. 5*A* (WT) and *B* (D224E) shows that at low P_i (0.01 mM) they are similar. The upward deflection with increasing hyperpolarization results from a block of P_i-sensitive leak current in oocytes expressing NaPi-IIa [2, 25]. When the P_i-concentration was increased D224E-mediated currents acquired a more prominent curvature than the WT. A similar pattern was seen when P_i was kept constant and Na^+ was varied (Fig. 5*D* and *E*). Extracting K_mP_i from the data of Fig. 5*A* and *B* using Eq. 1 and plotting it against V_m in Fig. 5*C* shows that K_mP_i for D224E was strongly voltage-dependent. K_mP_i was also significantly reduced, compared to WT, throughout the measurable range. Extracting the K_mNa values from the data in Fig. 5*D* and *E* using Eq. 1 (*H* constrained to 2.0) and plotting it against V_m in Figure 5F revealed that for D224E, K_mNa was strongly voltage-dependent, increasing over four-fold between −40 mV and −140 mV. For the WT, K_mNa was largely voltage-independent.

To see if P_i transport mediated by the D224G mutant was Na^+ dependent, we measured $^{32}P_i$ uptake in the presence and absence of external Na^+. As shown in Fig. 6*A*, P_i uptake in oocytes expressing WT and D224G was abolished in the absence of Na^+. To ascertain if Na^+ is also transported by D224G and to establish the Na:P_i stoichiometry, we performed simultaneous uptake of ^{22}Na and $^{32}P_i$ (Fig. 6*B*). Na^+ uptake measured in the absence of P_i shows that Na^+ uptake was low compared to the Pi-induced Na^+ uptake (Fig. 6*B* inset). For the WT, a linear regression line was fitted to the data with a slope of 2.7 ± 0.04, in agreement with a Na:P_i stoichiometry of 3:1, as previously reported [7, 25]. For D224G, the slope of the regression line was 10 ± 0.8, implying that 10 Na^+ ions were transported with each P_i. In the absence of detectable P_i-induced currents, the results indicated that D224G mediated significant P_i-dependent non-stoichiometric Na^+ transport, possibly Na^+-Na^+ exchange.

Asn-227

Given that oxygen-containing residues may play a role in coordinating Na^+ ions, as has been proposed for the Na-K-ATPase [20], we decided to carry out additional mutagenesis at Asn-227, a residue located one turn away from Asp-224 in the putative α-helical TMD-3. Replacing Asn with the negatively charged Asp (N227D) led to a poorly expressed construct that was unable to mediate significant P_i uptake (Fig. 7*A* and *B*). However, when Asn was replaced with Gln (N227Q), the construct expressed well and mediated significant P_i uptake (Fig. 7*A* and *B*) and P_i-induced currents (Fig. 7*C*). The apparent P_i and Na^+ affinities determined at −50 mV were markedly decreased compared to WT. Figure 7*D* shows a plot of the P_i-induced current as a function of the P_i concentration, normalized to $I_{Pi,\,max}$. The data were fitted with Eq. 1 ($H = 1$). K_mP_i for N227Q was 4.2 ± 1.7 mM, compared to 0.096 ± 0.011 mM for WT. We then

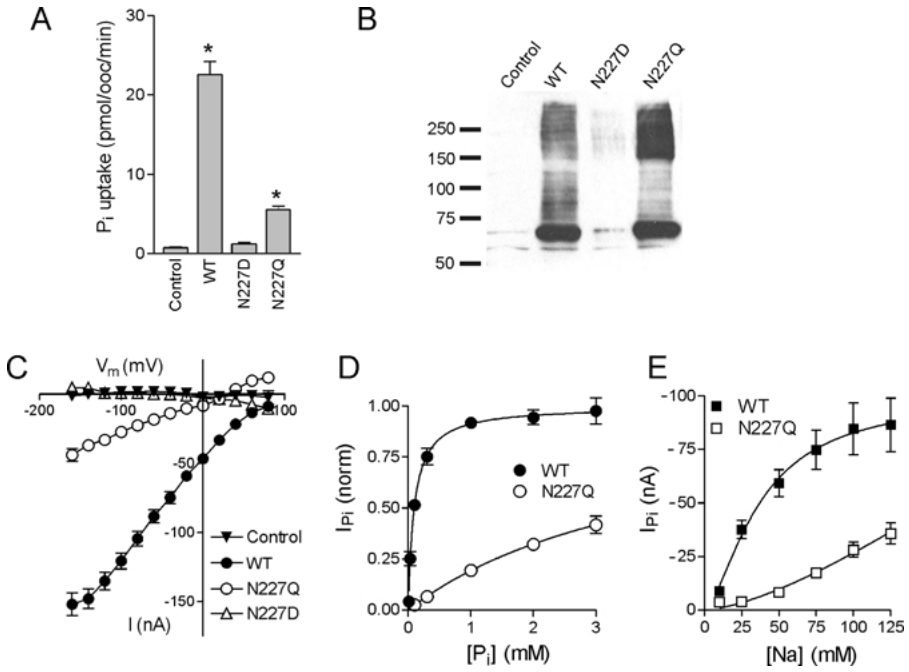

Fig. 7. Mutants at Asn-227. (*A*) P_i uptake. P_i uptake, using $^{32}P_i$ as a tracer, was measured in control oocytes and oocytes expressing mutant engineered at N227 in NaPi-IIa. Asterisk * denotes statistically significant difference from control ($P < 0.05$). (*B*) Western blot. Whole-cell lysates from oocytes expressing WT or mutant NaPi-IIa were probed with a NaPi-IIa-specific antibody. The size of the molecular weight markers is indicated in the figure. (*C*) Current-voltage relationships. P_i-induced currents were plotted against membrane potential in control oocytes and oocytes expressing WT or mutant NaPi-IIa. *Filled circles*, WT; *empty circles*, N227Q; *empty triangles*, N227Q; *filled triangles*, control. (*D*) K_mP_i of N227Q. Currents were acquired continuously at a holding potential of −50 mV. The current deflections induced by P_i application were plotted as a function of the P_i concentration as fitted with Eq. 1. The data were normalized to $I_{Pi,\ max}$. K_mP_i for WT was 0.096 ± 0.011 mM, for N227Q 4.2 ± 1.7 mM; $n = 6$. (*E*) K_mNa of N227Q. The current deflections induced by 3 mM P_i at different Na^+ concentrations were plotted as a function of the Na^+ concentration as fitted with Eq 1. For the WT, $K_mNa = 37 \pm 14$, $I_{Pi,\ max}$ 100 ± 20, $H = 1.6 \pm 0.6$. For N227Q, a reliable fit of Eq 1 to the data was prevented by the lack of saturation, but indicates a K_mNa of > 100 mM; $n = 4$–5.

attempted to estimate K_mNa for N227Q with 3 mM P_i, however, lack of saturation precluded a reliable estimate. The fit shown in Fig. 7*E* suggests for N227Q a $K_mNa > 100$ mM.

The P_i-induced current response in N227Q differed from that of the WT with a current reversal potential observed at around +40 mV (Fig. 7*C*). Removal of external Cl^- (replaced by glucuronate) had no effect on the outward current, indicating that it is not carried by inward movement of Cl^- ions (*data not shown*).

Glu-238

In the helical wheel TMD-3 representation (Fig. 1*C*), Glu-238 lies on the same face of a putative α-helix as Asp-224 and Asn-227. It is the only other charged residue in TMD-3 besides Asp-224 and highly conserved, and replacing it with a Cys resulted in a very poorly expressed construct for which we could measure neither $^{32}P_i$ transport nor P_i-induced currents (Fig. 3*A*). We therefore decided to explore this site further by mutating it to an Asp or a Gln. Both E238D and E238Q mediated P_i-induced currents that were ~50% of WT (*data not shown*). However, the substrate affinities were reduced. For E238D, K_mP_i was 0.24 ± 0.06 and K_mNa was 69 ± 4 mM, whereas for E238Q K_mP_i was 0.15 ± 0.03 and K_mNa 75 ± 5 ($n = 4$). This compares to a K_mP_i of 0.091 ± 0.022 and K_mNa of 34 ± 5 mM for the WT.

Discussion

In this study we have employed two approaches (SCAM and site-directed mutagenesis) to elucidate novel structure-function relationships of the predicted 3rd trasnsmembrane domain (TMD-3) of the human NaPi-IIa transporter. Previous studies in which we have applied SCAM to the rat NaPi-IIa, have focussed on the predicted linker regions (*see* Fig. 1*A*) ECL-1, ECL-4 [2, 3], ECL-3 [15] and ICL-1 [10]. The choice of TMD-3, as the first TMD to be investigated, was based on its proximity to ICL-1, which we propose has re-entrant properties and may form part of the substrate translocation pathway [10] and the presence of sites of potential importance in coordinating Na^+ ions [19, 20].

SCAM Suggests that TMD-3 Is not Readily Accessible from the Extracellular Aqueous Milieu

Ideally, when carrying out cysteine accessibility studies, it would be advantageous to remove all (13) native Cys, which otherwise might react with SH-reactive reagents. However, work on the rat NaPi-IIa isoform has shown that removing a number of the native Cys markedly reduces functional P_i cotransport expressed in *Xenopus* oocytes [12], making these constructs problematic to work with. Fortunately, none of the native Cys in WT NaPi-IIa are accessible to membrane-impermeant MTS reagents [12, 13]. We therefore decided to remove only Cys-225, the one native cysteine in putative TMD-3, before proceeding with SCAM, both as a precaution against possible disulfide bridge formation within the TMD-3 stretch or that mutagenesis in TMD-3 might cause Cys-225 to become MTS-reactive. The C225S mutant showed a ~50% decrease in P_i transport activity compared to WT, a reduction similar to that previously observed for the rat isoform [13]. Otherwise, this mutant exhibited transport characteristics similar to WT NaPi-IIa, which confirmed its suitability as a SCAM backbone.

Introducing novel Cys residues on a C225S background resulted in reduced or completely abolished P_i transport activity for all mutants except F226C-C225S. The Western blots shown in Fig. 3*B* indicate that in most cases this correlated with reduced protein expression in the oocyte. The notable exception is D224C-C225S, where the signal on the Western blot was as strong as for the WT, but neither P_i-induced currents nor P_i transport were detected. Also Cys substitution at polar/charged Asn-227 and Glu-238, lying on the same face of the putative α-helix (Fig. 1*C*), resulted in lack of P_i transport activity in spite of detectable protein expression. Interestingly, the only mutant with an increased K_mP_i, namely S230C-C225S, is found on the same side of a putative α-helix as D224, Asn-227 and E-238. The implications of these findings are discussed further below.

Unlike our previous SCAM studies on linker regions, where accessibility was readily determined experimentally in terms of altered transport function, only one double mutant in the present study (A240C-C225S) was functionally modified by MTS reagents. For this mutant, MTSEA or MTSET treatment reduced P_i-induced currents by ~50%. It is not clear why MTS reagents only partially blocked I_{Pi} in this mutant. Unfortunately the currents were too low after MTS modification to allow us to determine whether the P_i or Na^+ affinities or the turnover rate of the transporter had been altered by the modification. Nevertheless, its modified behavior indicated that the top of TMD-3 is accessible from the extracellular milieu, which confirmed the topological predictions for this motif. The negative findings for the other mutants suggest that the remainder of TMD-3 is buried within the protein, at least under the labelling conditions we employed (100 mM Na^+, −50 mV holding potential). Alternatively, the residues were indeed labelled without detectable change of function, however, this seems unlikely, given that mutagenesis at several of these sites (*see* below) resulted in dramatic changes in their electrogenic characteristics. Unfortunately, the low expression levels of most Cys mutants precluded a biochemical confirmation of labelling by using MTS-biotin, as we have previously reported for Cys mutants engineered in the loop regions of the rat NaPi-IIa isoform [3, 14].

Sites on the Hydrophilic Face of TMD-3 Are Critical Determinants of Electrogenicity and Substrate Interaction

Oxygen atoms are important in coordinating metal ions in proteins [19, 20, 24], which suggests that they could also be important in forming a binding site for Na^+ ions in NaPi-IIa. Moreover, it is significant that TMD-3 contains three oxygen-containing residues all located on the same hydrophilic face of the helical wheel representation of TMD-3. Mutagenesis at Asp-224 had profound effects on the P_i transport function of NaPi-IIa. The most notable mutation was D224G where we replaced Asp, a residue conserved in all electrogenic type IIa and IIb transporters, with Gly that appears at the equivalent position in electroneutral NaPi-IIc. D224G mediated low, but significant Na^+-dependent P_i uptake. The amount of Na^+-dependent P_i uptake in Fig. 6*A* corresponded to ~10 nA of current (assuming that one charge is transported per P_i), which is well above the detection limit of our system. Since we were unable to detect any P_i-induced currents in D224G-expressing oocytes, the result showed that this single point mutation was able to convert an electrogenic transporter into an electroneutral one. This suggests that the carboxylic acid side chain of Asp-224 may participate in forming a binding site for one of the three Na^+ ions transported by NaPi-IIa per transport cycle, and its removal compromised this binding site. This hypothesis is strengthened by the observation that a triple-mutation of electroneutral NaPi-IIc (S187A-S191A-G195D), in which the Gly of NaPi-IIc at the position equivalent to Asp-224 in NaPi-IIa was changed to Asp, is electrogenic and operates with a 3:1 Na:P_i stoichiometry, in contrast to the 2:1 stoichiometry of the WT NaPi-IIc [1]. However, the D224G mutation alone was not sufficient to recreate the full kinetic profile of the NaPi-IIc WT, as shown by the large P_i-induced Na^+ leak (Fig. 6*B*).

The importance of the length of the carboxylic side chain of Asp-224 for NaPi-IIa electrogenicity

was further underscored by the altered voltage dependency of P_i-induced currents by D224E, and the dramatically altered voltage dependency of K_mNa (Fig. 5*F*). For D224E the apparent Na^+ affinity was larger than that of the WT at V_m more positive than −60 mV, but decreased and became lower than that of the WT at potentials more negative than −80 mV. Additionally the apparent P_i affinity was strongly decreased at hyperpolarizing potentials, but as K_mNa was measured at saturating P_i (1 mM) throughout the voltage range, whereas K_mP_i was not (100 mM Na^+; oocytes did not tolerate prolonged exposure to hyperosmotic solutions); the effect of voltage on K_mP_i could, at least partially, be secondary to its effect on K_mNa.

Asn-227, which is located one turn further along the α-helical TMD-3, may also play a significant role in the transport function of NaPi-IIa. Substitution with Cys (N227C-C225S) resulted in a construct unable to mediate functional P_i uptake in oocytes. However, protein expression was also low, so the absence of P_i transport may have been due to impaired expression. This was also most likely the case for N227D, where the polar amine group of Asn was substituted with the charged carboxyl of Asp. However, when we replaced Asn with the polar, but slightly longer Gln, the resulting construct expressed well and mediated electrogenic P_i transport, albeit with considerably reduced Na^+ and P_i affinities. Interestingly, a similar phenotype was reported for mutagenesis at Asn-199 in the predicted ICL-1 (marked with a grey circle in Fig. 1*A*). At this site, substitution with Cys as well as shorter polar (Thr) or non-polar (Ala) side chains resulted in reduced apparent substrate affinities, whereas substitution of larger or charged residues (Asp, His, Gln, Arg) resulted in fully suppressed cotransport function [10]. Taken together, our present findings suggest that Asn-227 also contributes to the substrate binding site and may be in close proximity to Asn-199 in ICL-1.

Ser-230 lies a further turn along TMD-3. Interestingly, S230C-C225S expressed well but this was the only mutant to show a significantly reduced apparent P_i and Na^+ affinity compared to the C225S alone. One explanation for this behavior is that substitution of polar Ser with less polar Cys may impede the movement of Na^+ towards its putative binding site further down this amphipathic helix. Finally, Glu-238, lying a further two turns along the α-helix, is the only other charged residue of TMD-3. Cys substitution at this site was not tolerated, but substitution with the charged Asp or polar Gln resulted in functional mutants that mediated electrogenic P_i transport with reduced substrate affinities.

Taken together, the results of the Cys scanning mutagenesis and the additional mutagenesis of Asp-224, Asn-227, Ser-230 and Glu-238 are consistent with TMD-3 forming an amphipathic helix that contains important elements for substrate binding.

Conclusions

This is the first study describing cysteine scanning mutagenesis in a NaPi-IIa protein TMD. An introduced Cys located at the predicted top (extracellular) end of TMD-3 could be functionally modified using MTS reagents, confirming the predicted topology and suggesting that the remainder of TMD-3 is largely buried in the membrane. Additional mutagenesis at Asp-224 identified this residue to be critical for electrogenic P_i transport in NaP_i-IIa, and this has been recently confirmed by mutagenesis at the equivalent site in the electroneutral mouse NaPi-IIc [1]. The amphipathic nature of the α-helical segment of TMD-3 and the effect of mutagenesis on polar or charged amino acids clustering on one side of the helix indicate that this region participates in forming a binding site for a sodium ion and is critical for establishing the 3:1 Na^+:P_i stoichiometry required for electrogenic Na^+-coupled P_i cotransport.

This work was supported by grants from the Swiss National Science Foundation, the Gebert Rüf Stiftung, the Hartmann-Müller Stiftung (Zürich), the Fridericus Stiftung (Vaduz), the Olga Mayenfish-Stiftung (Zürich) and the Union Bank of Switzerland.

References

1. Bacconi, A., Virkki, L.V., Biber, J., Murer, H., Forster, I.C. 2005. Renouncing electrogenicity is not free of charge: switching on electrogenicity in a Na+-coupled J phosphate cotransporter. *Proc. Natl. Acad. Sci. USA* **102:**12606–12611
2. Ehnes, C., Forster, I.C., Bacconi, A., Kohler, K., Biber, J., Murer, H. 2004. Structure-function relations of the first and fourth extracellular linkers of the type IIa Na^+/P_i cotransporter: II. Substrate interaction and voltage dependency of two functionally important sites. *J. Gen. Physiol.* **124:**489–503
3. Ehnes, C., Forster, I.C., Kohler, K., Bacconi, A., Stange, G., Biber, J., Murer, H. 2004. Structure-function relations of the first and fourth predicted extracellular linkers of the type IIa Na^+/Pi cotransporter: I. Cysteine scanning mutagenesis. *J. Gen. Physiol.* **124:**475–488
4. Feild, J.A., Zhang, L., Brun, K.A., Brooks, D.P., Edwards, R.M. 1999. Cloning and functional characterization of a sodium-dependent phosphate transporter expressed in human lung and small intestine. *Biochem. Biophys. Res. Commun.* **258:**578–582
5. Forster, I., Hernando, N., Biber, J., Murer, H. 1998. The voltage dependence of a cloned mammalian renal type II Na^+/P_i cotransporter (NaPi-2). *J. Gen. Physiol.* **112:**1–18
6. Forster, I.C., Kohler, K., Biber, J., Murer, H. 2002. Forging the link between structure and function of electrogenic cotransporters: the renal type IIa Na^+/P_i cotransporter as a case study. *Prog. Biophys. Mol. Biol.* **80:**69–108
7. Forster, I.C., Loo, D.D., Eskandari, S. 1999. Stoichiometry and Na^+ binding cooperativity of rat and flounder renal type II Na^+-P; cotransporters. *Am. J. Physiol.* **276:**F644–F649

8. Hayes, G., Busch, A., Lotscher, M., Waldegger, S., Lang, F., Verrey, F., Biber, J., Murer, H. 1994. Role of N-linked glycosylation in rat renal Na/Pi-cotransport. *J. Biol. Chem.* **269:**24143–24149
9. Hilfiker, H., Hattenhauer, O., Traebert, M., Forster, I., Murer, H., Biber, J. 1998. Characterization of a murine type II sodium-phosphate cotransporter expressed in mammalian small intestine. *Proc. Natl. Acad. Sci. USA* **95:**14564–14569
10. Kohler, K., Forster, I.C., Stange, G., Biber, J., Murer, H. 2002. Identification of functionally important sites in the first intracellular loop of the NaPi-IIa cotransporter. *Am. J. Physiol.* **282:**F687–F696
11. Kohler, K., Forster, I.C., Stange, G., Biber, J., Murer, H. 2002. Transport function of the renal type IIa Na^+/P_i cotransporter is codetermined by residues in two opposing linker regions. *J. Gen. Physiol.* **120:**693–703
12. Kohler, K., Forster, I.C., Stange, G., Biber, J., Murer, H. 2003. Essential cysteine residues of the type Iia Na^+/P_i cotransporter. *Pfluegers Arch.* **446:**203–210
13. Lambert, G., Forster, I.C., Biber, J., Murer, H. 2000. Cysteine residues and the structure of the rat renal proximal tubular type II sodium phosphate cotransporter (rat NaPi IIa). *J. Membrane Biol.* **176:**133–141
14. Lambert, G., Forster, I.C., Stange, G., Biber, J., Murer, H. 1999. Properties of the mutant Ser-460-Cys implicate this site in a functionally important region of the type IIa Na^+/P_i cotransporter protein. *J. Gen. Physiol.* **114:**637–652
15. Lambert, G., Forster, I.C., Stange, G., Kohler, K., Biber, J., Murer, H. 2001. Cysteine mutagenesis reveals novel structure-function features within the predicted third extracellular loop of the type IIa Na^+/P_i cotransporter. *J. Gen. Physiol.* **117:**533–546
16. Lambert, G., Traebert, M., Hernando, N., Biber, J., Murer, H. 1999. Studies on the topology of the renal type II NaPi-cotransporter. *Pfluegers Arch.* **437:**972–978
17. Murer, H., Forster, I., Biber, J. 2004. The sodium phosphate cotransporter family SLC34. *Pfluegers Arch.* **447:**763–767
18. Murer, H., Hernando, N., Forster, I., Biber, J. 2000. Proximal tubular phosphate reabsorption: molecular mechanisms. *Physiol. Rev.* **80:**1373–1409
19. Nayal, M., Di Cera, E. 1994. Predicting Ca^{2+}-binding sites in proteins. *Proc. Natl. Acad. Sci. USA* **91:**817–821
20. Ogawa, H., Toyoshima, C. 2002. Homology modeling of the cation binding sites of Na^+K^+-ATPase. *Proc. Natl. Acad. Sci. USA* **99:**15977–15982
21. Ohkido, I., Segawa, H., Yanagida, R., Nakamura, M., Miyamoto, K. 2003. Cloning, gene structure and dietary regulation of the type-IIc Na/Pi cotransporter in the mouse kidney. *Pfluegers Arch.* **446:**106–115
22. Segawa, H., Kaneko, I., Takahashi, A., Kuwahata, M., Ito, M., Ohkido, I., Tatsumi, S., Miyamoto, K. 2002. Growth-related renal type II Na/Pi cotransporter. *J. Biol. Chem.* **277:**19665–19672
23. Tenenhouse, H.S., Murer, H. 2003. Disorders of renal tubular phosphate transport. *J. Am. Soc. Nephrol.* **14:**240–248
24. Toyoshima, C., Nakasako, M., Nomura, H., Ogawa, H. 2000. Crystal structure of the calcium pump of sarcoplasmic reticulum at 2.6 A resolution. *Nature* **405:**647–655
25. Virkki, L.V., Forster, I.C., Biber, J., Murer, H. 2005. Substrate interactions in the human type IIa sodium-phosphate cotransporter (NaPi-IIa). *Am. J. Physiol.* **288:**F969–F981
26. Virkki, L.V., Forster, I.C., Hernando, N., Biber, J., Murer, H. 2003. Functional characterization of two naturally occurring mutations in the human sodium-phosphate cotransporter type IIa. *J. Bone Miner. Res.* **18:**2135–2141
27. Werner, A., Biber, J., Forgo, J., Palacin, M., Murer, H. 1990. Expression of renal transport systems for inorganic phosphate and sulfate in *Xenopus laevis* oocytes. *J. Biol. Chem.* **265:**12331–12336